JOURNAL OF PROPULSION AND POWER
Vol. 11, No. 6, November–December 1995

Shock-Wave/Boundary-Layer Interactions with Bleed Part 2: Effect of Slot Location

A. Hamed,* J. J. Yeuan,† and S. H. Shih‡
University of Cincinnati, Cincinnati, Ohio 45221

The effect of bleed configuration in the interaction region of an oblique shock wave and a turbulent boundary layer was investigated using numerical simulations. The numerical solutions to the compressible Navier–Stokes equations reveal the flow details throughout the interaction zone and inside the slanted and normal bleed slots. Different bleed mass flow rates up to 16% of the incoming boundary layer are obtained by changing the plenum pressure. Results are presented for an incident oblique shock of sufficient strength to cause boundary-layer separation in the absence of bleed. The results show the flow characteristics including an expansion/compression wave system across the slot opening and recirculation zone inside the slot. The performance of the different bleed configurations is compared in terms of the discharge coefficient and the boundary-layer characteristics downstream of the interaction, at the different bleed mass flow rates.

Introduction

AIR bleed systems are used for controlling the shock-wave/boundary-layer interactions when operating at supersonic speeds. Proper bleed system design is particularly important for the efficient and stable operation of mixed compression supersonic inlets.[1] The fundamental objectives of supersonic inlet bleed system design are to provide good aerodynamic flow characteristics with minimum boundary-layer bleed.[2,3] Bleed is required in the regions of oblique shock reflections with strong adverse pressure gradients to prevent excessive deterioration of the inlet boundary-layer profiles.[4] Meeting the supersonic inlet performance requirements is achieved through the optimization of bleed system design. This requires a knowledge of the effect of bleed mass flow, location, and geometry on the supersonic inlet boundary layer. Comparisons of internal flow computational results[5–7] with experimental measurements in supersonic inlets[7,8] revealed reasonable agreement between the computed and measured surface pressures upstream of the ramp bleed. However, discrepancies in the predicted shock locations and velocity profiles were observed downstream of shock-wave/boundary-layer interactions with bleed.

Hamed and Shang[1] reviewed the existing experimental data base for shock-wave/boundary-layer interactions in supersonic inlets and other related configurations. According to this survey, there is enough experimental evidence[9–14] to indicate that local bleed can control flow separation in shock-wave/boundary-layer interactions. There are disagreements,[1] however, among the different experimental results regarding the effects of bleed location relative to the shock.[9–12] Strike and Rippy[9] measured the surface pressure in the interaction zone of an oblique shock wave impinging on a turbulent boundary layer over a flat plate with suction. They determined that less suction is required to control separation when applied upstream of the shock. Seebaugh and Childs[10] investigated experimentally the axisymmetric flow in the interaction region of the boundary layer inside a duct. Contrary to the conclusions of Strike and Rippy,[9] suction within the interaction region was found to be more effective in suppressing the effects of separation than suction applied upstream. Hamed et al.[15–18] modeled bleed by resolving the flow through the individual bleed ports in the flowfield computations of compressible viscous flows. The effect of slant angle on the bleed performance when applied across the shock impingement point was presented in Part 1. The bleed discharge coefficient was found to increase with decreased bleed port slant angle due to the reduction in the extent of the recirculating flow zone inside the slot. Furthermore, the friction coefficient over the slot surface downstream of the interaction could be increased by 20% with bleed through normal slot and by 40% for bleed through the slanted slot compared to the no-bleed case.

As a result of the findings in Part 1, the 20- and 90-deg bleed slots were selected for further investigation to study the effect of bleed location relative to the shock impingement. Flow predictions were obtained through the interaction region and inside the slot using the PARC code[19] with the k-ε turbulence model. The flowfield characteristics were determined at different bleed mass flows up to 60% of the incoming boundary-layer mass flow by varying the slot width and the static pressure at the bottom of the slot.

Computational Details

Numerical flow simulations were conducted for bleed applied through normal and slanted slots in the interaction region of an externally generated incident oblique shock and a turbulent boundary layer. The flow was considered to be turbulent throughout the calculation domain; no attempt was made to model transition and/or relaminarization. The solution domain used in the two-dimensional flow simulations extends upstream of the flat plate leading edge, downstream of the interaction region, and inside the bleed slot, where the specified plenum pressure at the bottom of the slot controlled the amount of bleed mass flow.

The upper solution domain boundary was set at 0.13 ft from the flat plate with the lower solution domain at the bottom of the bleed slot. In the streamwise direction, the domain extended along the plate length of 1.13 ft and the distance of 0.07 ft, upstream of the plate leading edge to the station where the uniform upstream conditions are applied. The computational grid and the boundary conditions used were the same as outlined in Ref. 20.

Presented as Paper 93-2992 at the AIAA 24th Fluid Dynamics Conference, Orlando, FL, July 6–9, 1993; received Aug. 6, 1994; revision received Jan. 27, 1995; accepted for publication Feb. 11, 1995.

*Professor, Department of Aerospace Engineering and Engineering Mechanics. Fellow AIAA.

†Postdoctoral Assistant, Department of Aerospace Engineering and Engineering Mechanics. Member AIAA.

‡Student, Department of Aerospace Engineering and Engineering Mechanics. Student Member AIAA.

Results and Discussion

The computations were conducted at the incoming flow conditions of $M = 2.96$, $Re = 1.2 \times 10^7$/ft, and an impinging oblique shock angle of 25.84 deg (wedge angle of 7.93 deg), which causes separated flow if no bleed is applied. The flow characteristics inside the bleed slot and throughout the interaction were determined for bleed through a normal and 20-deg slanted slot. The slot width along the plate surface for the normal bleed case was 0.01065 ft, which is equal to 0.8085 times the boundary-layer thickness upstream of the interaction. To maintain comparable bleed mass flows among the normal and slanted bleed cases the opening at the plate surface was maintained at 0.01065 ft, leading to a 20-deg slot width, which is 0.2766 times the boundary layer upstream of the interaction. The effect of bleed location was investigated by studying the flowfield with bleed applied upstream, across, and downstream of the incident shock interaction with the

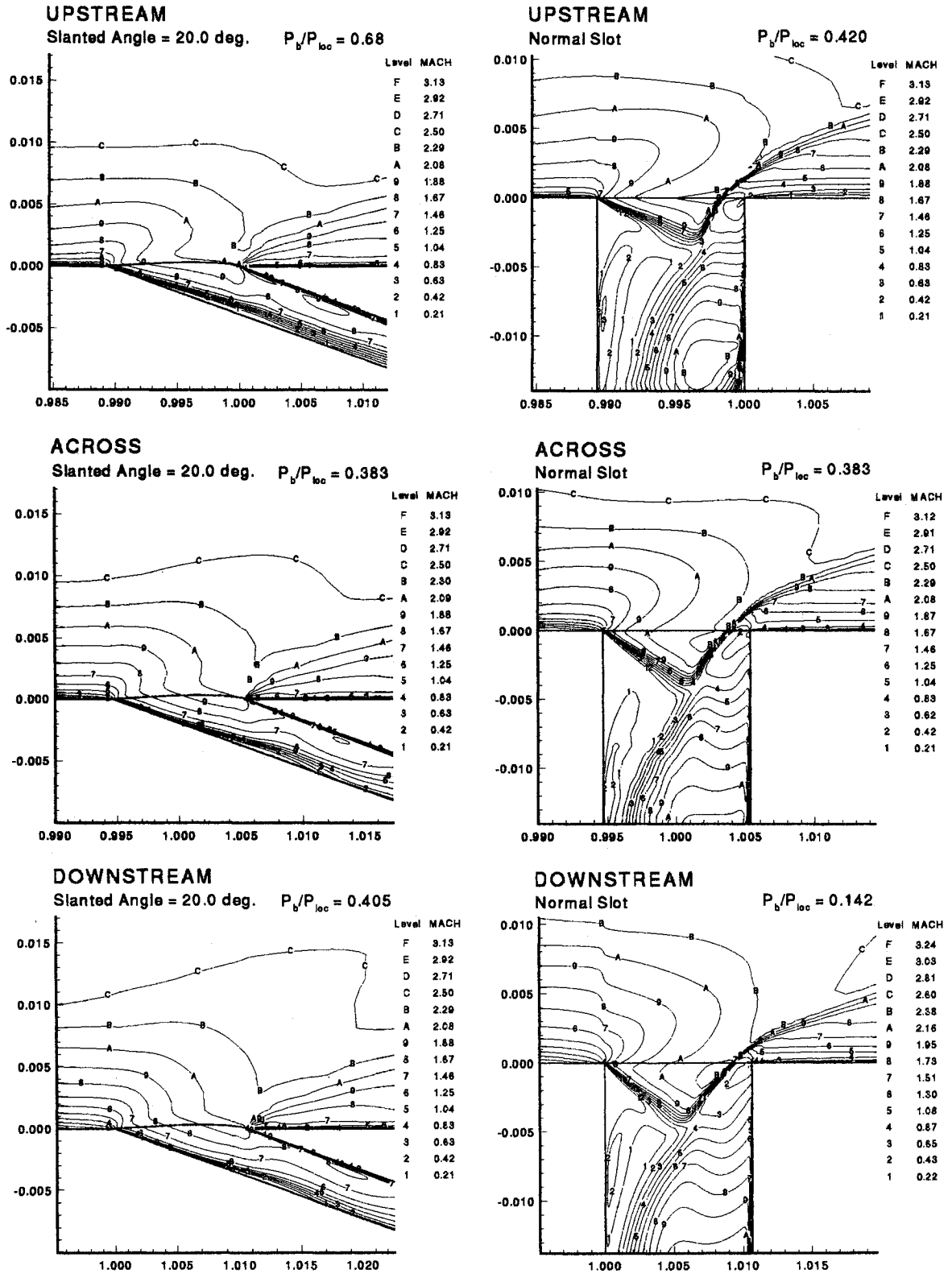

Fig. 1 Mach number contours for four different slot geometries at choked conditions.

plate surface. The slot opening center X_{ref} was located at 0.99468, 1.0, and 1.00532 ft from the plate leading edge for the three cases, respectively. This corresponds to the incident shock interaction point with the plate situated at the downstream corner, the center, and the upstream corner, respectively, for the three bleed locations.

Figure 1 presents the Mach number contours for the six different slot geometries at choked conditions. The corresponding Mach number and flow angle distribution across the slot opening are presented in Figs. 2 and 3. The static pressure and friction coefficient distribution over the plate surface are presented in Figs. 4 and 5. In Figs. 2–5, the results for the three different bleed locations were shifted such that they were all aligned around the center of the bleed opening X_{ref} in each case. The wave system across the bleed opening and the recirculation flow region inside the slot at the upstream wall were discussed in Part 1. The flow angle is equal to the slot angle in the 20-deg slanted bleed, but is less than 40 deg in the case of normal bleed. The initial sharp flow overturning in the normal bleed case (Fig. 3) is caused by a small separation bubble on the plate surface upstream of the slot, which is confirmed by the negative friction in Fig. 5a. According to Figs. 1 and 3, the flow turning through expansion at the normal slot's opening increases as the slot location moves downstream. According to Fig. 2, the Mach number across the 20-deg slot opening is initially higher in the upstream bleed case, but approaches the same value towards the slot's downstream corner as the other two bleed locations. According to Fig. 5, a small separated flow region is predicted upstream of the

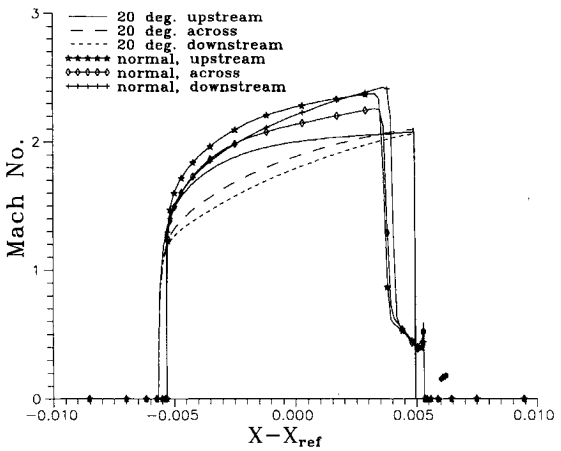

Fig. 2 Mach number distribution across the slot opening at choked conditions.

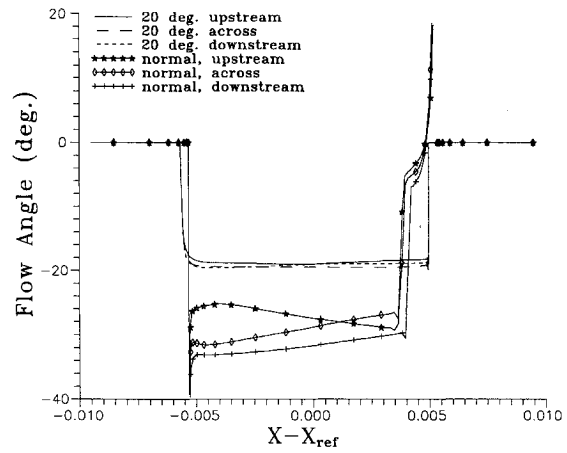

Fig. 3 Flow angle distribution across the slot opening at choked conditions.

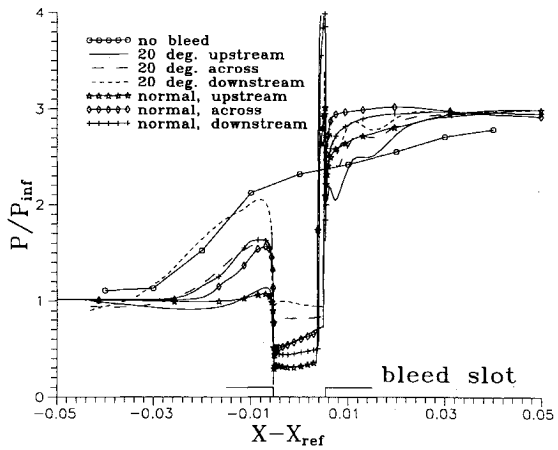

Fig. 4 Static pressure distribution across the slot opening at choked conditions.

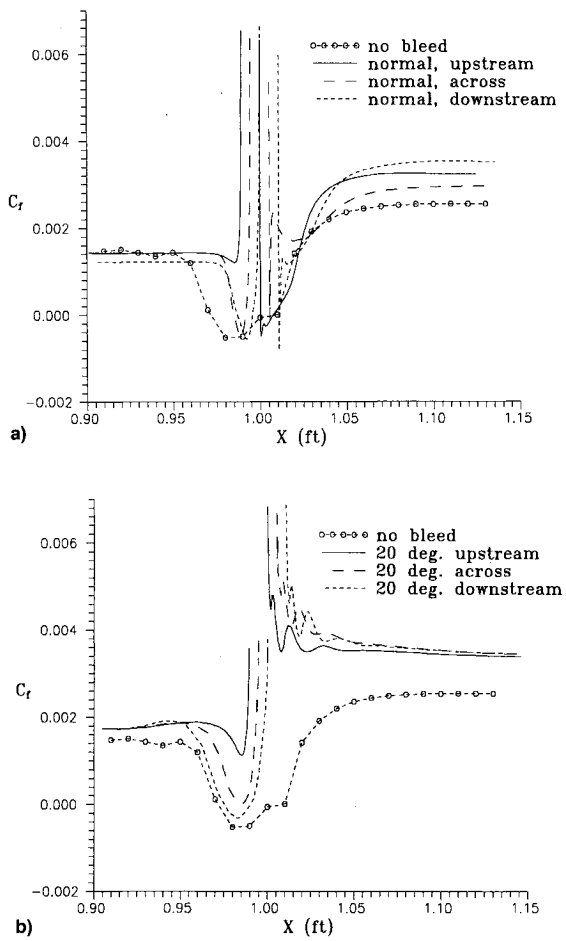

Fig. 5 Friction coefficient distribution in the interaction region at choked conditions.

normal slot and an even smaller one at the downstream corner in all normal bleed cases. On the other hand, no flow separation was predicted over the plate surface with the 20-deg slanted bleed slot, except in the case of bleed downstream of the shock where the flow separates upstream of the slot opening. Figures 4 and 5 show that the mass removal effects extend both upstream and downstream of the bleed slot and are reflected in both the surface pressure and friction coefficient. The fastest pressure rise downstream of the bleed slot is observed in the case of normal bleed across the shock and the slowest in the case of slanted bleed upstream of the shock.

The change in the friction coefficient over the plate surface downstream of the interaction is characteristically that of boundary layer redeveloping in the case of bleed through the slanted slots[20] and is slightly higher when the bleed is applied further downstream. The skin friction distribution increases downstream of the interaction in the case of normal bleed since the stagnation point is slightly inside the slot's downstream wall. Normal bleed downstream of the shock results in higher friction coefficient followed by upstream then across the shock.

Figure 6 presents the variation in the slot discharge coefficient with the plenum pressure P_b normalized by the local pressure P_{loc}. For the bleed locations upstream, across, and downstream, P_{loc} represents the pressure before the incident shock ($P_{loc} = 1.0P_{inf}$), behind the incident shock ($P_{loc} = 1.7752P_{inf}$), and behind the reflected shock ($P_{loc} = 2.96P_{inf}$), respectively. The same data are represented in Fig. 7 in the form of bleed mass flow as a percentage of the boundary-layer mass flow upstream of the interaction at $x = 0.9$ ft. According to these figures, the highest discharge coefficient is obtained with the upstream bleed through a 20-deg slot and the lowest with downstream through a normal slot. The slanted bleed discharge coefficient is very sensitive to the bleed location. Upstream bleed through a 20-deg slot results in the highest discharge coefficients, which is double that of downstream bleed at choked conditions. The choking bleed mass flow itself, however, is less sensitive to slanted bleed location, with upstream bleed choked mass flow only 25% higher than downstream. Bleed through normal slot results in much lower choked discharge coefficient, less than 50% that of the 20-deg slot downstream of the shock and less than 25% of the 20-deg slot upstream of the shock. There is a very small difference between the upstream and across the shock normal bleed cases, but the normal bleed downstream of the shock gives the lowest choked bleed discharge coefficient, which is 40% below the other two locations. According to Fig. 7, the bleed mass itself is higher for normal bleed downstream of the shock, but it decreases rapidly with increased plenum pressure.

The effect of bleed mass flow on the boundary-layer characteristics downstream of the interactions at $X = 1.13$ ft is presented in Figs. 8–11 for all six configurations. According

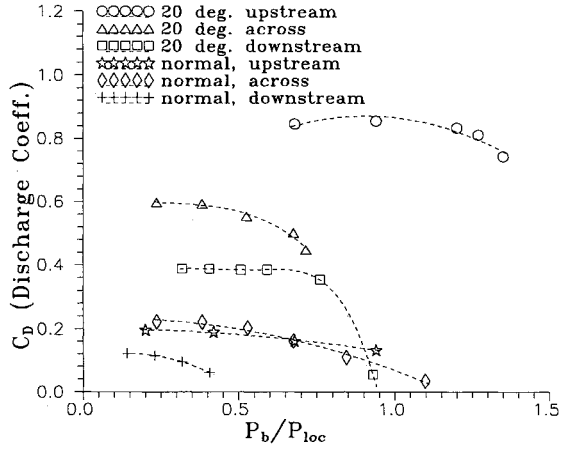

Fig. 6 Variation of discharge coefficient with the bleed plenum pressure.

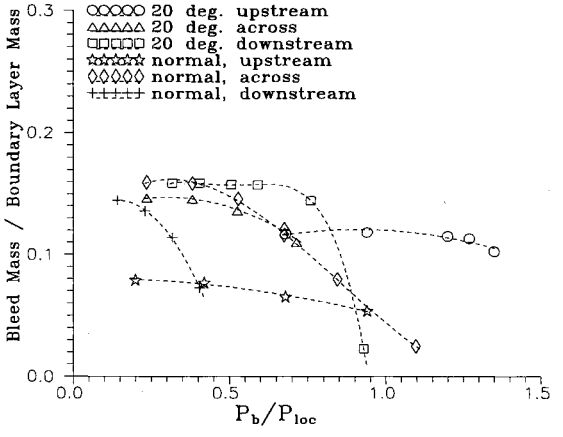

Fig. 7 Variation of bleed mass flow rate with the bleed plenum pressure.

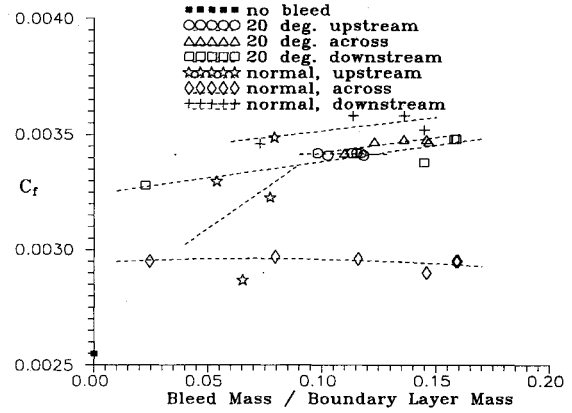

Fig. 8 Effect of bleed mass flow on the friction coefficient downstream of interaction region, at $x = 1.13$ ft.

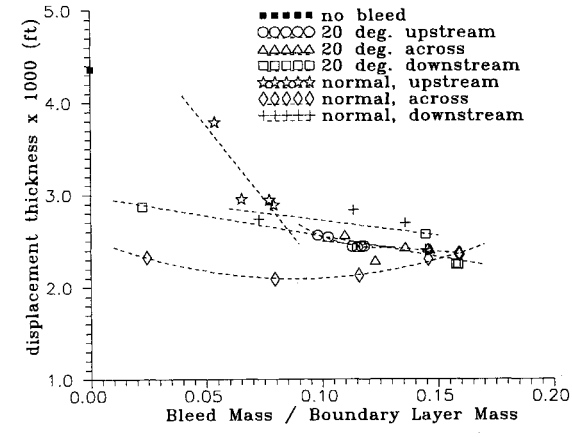

Fig. 9 Effect of bleed mass flow on the displacement thickness downstream of interaction region, at $x = 1.13$ ft.

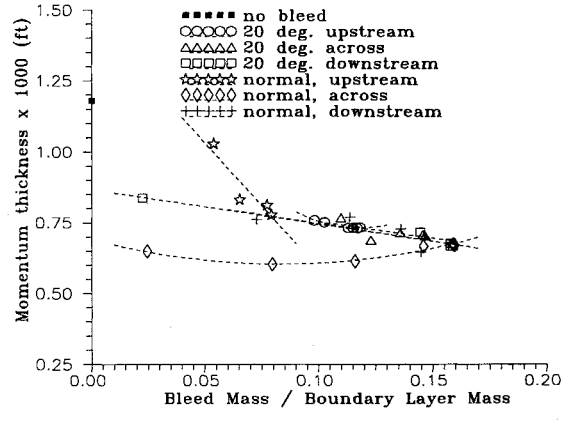

Fig. 10 Effect of bleed mass flow on the momentum thickness downstream of interaction region, at $x = 1.13$ ft.

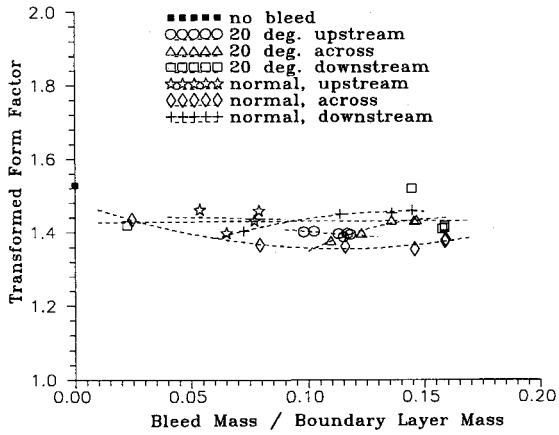

Fig. 11 Effect of bleed mass flow on the transformed form factor downstream of interaction region, at x = 1.13 ft.

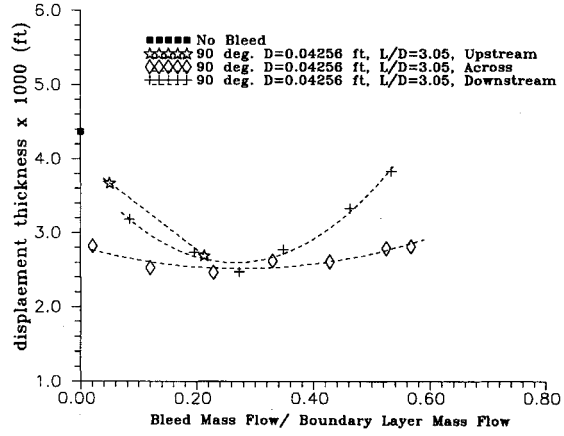

Fig. 12 Effect of bleed mass flow on the displacement thickness downstream of interaction region, at x = 1.13 ft.

to these figures, all slot configurations produce nearly the same displacement thickness δ^* = 0.0024 ft and momentum thickness θ = 0.0007 ft at choking, but the bleed through the normal slot across the shock produces lower values (δ^* = 0.0021 ft and θ = 0.0006 ft) at bleed mass flow rate values as low as 8% of the boundary layer. The transformed form factor downstream of the interaction had the smallest value (H_{tr} = 1.36) for the normal slot at a bleed mass flow rate equal to 15% of the boundary layer. Because of the small differences in the bleed slot locations (a maximum of 0.0106 ft or 0.8085 times the boundary-layer thickness upstream), additional results were obtained for wider normal slots whose centers were located at X = 0.97872, 1.0, and 1.04256 ft from the leading edge to gain a better understanding of the effect of bleed location relative to the shock and of bleed mass flow on the boundary-layer characteristics downstream. The resulting boundary-layer characteristics for these wide slots (D/δ = 3.234) are presented in Figs. 12 and 13. According to the results in these figures, all three configurations produce approximately the same effect at bleed mass flows equal to 28% of the coming boundary layer. The performance of the normal bleed slot downstream of the shock deteriorates with further increases in the bleed mass flow, causing both the displacement and momentum thickness to increase. Across the shock bleed generally produces larger reductions in both displacement and momentum thickness than either upstream or downstream bleeds. This is especially more evident at the lower bleed mass flows that are less than 20% of the incoming boundary layer. However, these large bleed mass flows with the wider normal slots do improve the downstream boundary-

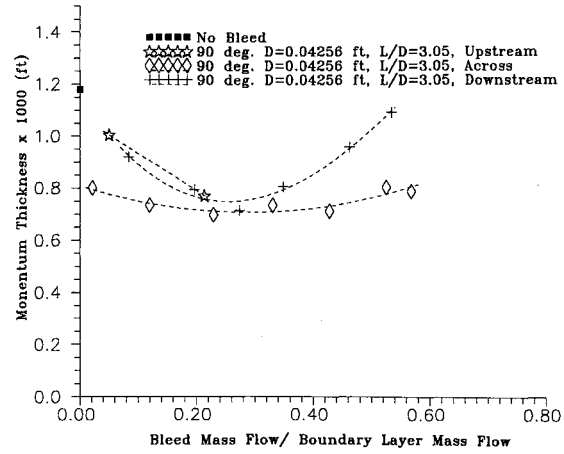

Fig. 13 Effect of bleed mass flow on the momentum thickness downstream of interaction region, at x = 1.13 ft.

layer characteristics compared to the small bleed mass flows through the narrow slots.

Conclusions

A numerical investigation was conducted to study the effect of a 20-deg slanted and normal bleed slot location relative to the shock on the flowfield in an oblique shock-wave/turbulent boundary-layer interaction. The results indicate that the slanted bleed slot discharge coefficient is more sensitive to bleed location and had the highest value when the slanted bleed slot was located upstream of the incident shock. From the six different bleed configurations with bleed mass flows up to 16% of the incoming boundary layer, the normal slot produced the highest friction coefficient downstream of the interaction when located downstream of the shock and the lowest friction coefficient when located upstream. For slanted slot bleed mass flows between 9–16% of the incoming boundary layer, the momentum and displacement thickness of the boundary layer downstream decreased with increased mass flow, but were insensitive to the slot location relative to the shock impingement pouch. At 26% of the incoming boundary-layer mass flow, the bleed through the three normal slots reduced the boundary-layer displacement and momentum thickness by 50%. A sharp deterioration in the effectiveness of normal bleed downstream of the shock in reducing δ^* and θ downstream was maintained over the range of bleed mass flow rates when the normal bleed slot was located across the shock impingement point. The smallest reduction in the δ^* and θ was obtained with normal upstream bleed and the largest reduction with the across the shock unchoked normal bleed. The effect of normal bleed slot width was investigated and the boundary-layer characteristics were more sensitive to bleed location for larger bleed mass flows up to 50% of the boundary-layer slots. In general, across the shock normal bleed resulted in larger reductions in both δ^* and θ, but all bleed locations were most effective and produced similar reductions when 26% of the incoming boundary layer was bled through the normal slots.

Acknowledgments

This work was sponsored by NASA Lewis Research Center, D. Saunders was the Project Monitor. The computational work was performed on the Cray Y-MP of the Ohio Supercomputer.

References

[1]Hamed, A., and Shang, J., "Survey and Assessment of the Validation Data Base for Shock Wave Boundary Layer Interactions in

Supersonic Inlets," AIAA Paper 89-2939, July 1989.

[2]Syberg, J., and Koncsek, J. L., "Bleed System Design Technology for Supersonic Inlets," AIAA Paper 72-1138, June 1972.

[3]Fukuda, M. K., Hingst, W. R., and Reshotko, E., "Bleed Effects on Shock/Boundary-Layer Interactions in Supersonic Mixed Compression Inlets," *Journal of Aircraft*, Vol. 14, No. 2, 1977, pp. 151–156.

[4]Hamed, A., "Flow Separation in Shock Wave-Bounday Layer Interactions at Hypersonic Speeds," NASA CR 4274, Feb. 1990.

[5]Martin, A. W., Koslin, L. C., and Sidney, D. M., "Dynamic Distortion at the Exit of a Subsonic Diffuser of a Mixed Compression Inlet," NASA CR-1644, Dec. 1970.

[6]Knight, D. D., "Improved Calculation of High Speed Inlet Flows Part 1: Numerical Algorithm," *AIAA Journal*, Vol. 19, No. 1, 1981, pp. 34–41; also "Improved Calculation of High Speed Inlet Flows Part 2: Results," *AIAA Journal*, Vol. 19, No. 2, 1981, pp. 172–179.

[7]Weir, L. J., Reddy, D. R., and Rupp, G. D., "Mach 5 Inlet CFD and Experimental Results," AIAA Paper 89-2355, July 1989.

[8]Carter, T. D., and Spong, E. D., "High Speed Inlet Investigation. Vol. I Description of Program and Results; Vol. II Data Summary," Air Force Flight Dynamics Lab., AFFDL-TR-77-105, Nov. 1977.

[9]Strike, W. T., and Rippy, J., "Influence of Suction on the Interaction of an Oblique Shock with a Turbulent Boundary Layer at Mach 3," Arnold Engineering Development Center, AEDC-TN-61-129, Oct. 1961.

[10]Seebaugh, W., and Childs, M., "Conical Shock Wave Boundary Layer Interaction Including Suction Effects," *Journal of Aircraft*, Vol. 7, No. 4, 1970, pp. 334–340.

[11]Benhachmi, D., Greber, I., and Hingst, W., "Experimental and Numerical Investigation of an Oblique Shock-Wave/Turbulent Boundary Layer Interaction with Continuous Suction," AIAA Paper 89-0357, Jan. 1989.

[12]Gubbison, R. W., Meleason, E. T., and Johnson, D. F., "Performance Characteristics from Mach 2.58 to 1.98 of an Axisymmetric Mixed Compression Inlet System with 60 Percent Internal Contraction," NASA TM X-1739, Feb. 1969.

[13]Fukuda, M. K., Hingst, W. G., and Reshotko, E., "Control of Shock Boundary Layer Interactions by Bleed in Mixed Compression Inlets," NASA CR 2595, May 1975.

[14]Wong, W. F., "The Application of Boundary Layer Suction to Suppress Strong Shock-Induced Separation in Supersonic Inlets," AIAA Paper 74-1063, Oct. 1974.

[15]Hamed, A., and Lehnig, T., "An Investigation of Oblique Shock/Boundary Layer/Bleed Interaction," *Journal of Propulsion and Power*, Vol. 8, No. 2, 1992, pp. 418–424.

[16]Hamed, A., and Lehnig, T., "The Effect of Bleed Configuration on Shock/Boundary Layer Interactions," AIAA Paper 91-2014, June 1991.

[17]Hamed, A., Shih, S. H., and Yeuan, J. J., "An Investigation of Shock/Turbulent Boundary Layer/Bleed Interaction," AIAA Paper 92-3085, Jan. 1992.

[18]Hamed, A., Shih, S. H., and Yeuan, J. J., "A Parametric Study of Bleed in Shock Boundary Layer Interactions," AIAA Paper 93-0294, Jan. 1993.

[19]Cooper, G. K., and Sirbaugh, J. R., "PARC Code: Theory and Usage," Arnold Engineering Development Center, AEDC-TR-89-15, Dec. 1989.

[20]Hamed, A., Yeuan, J. J., and Shih, S. H., "An Investigation of Shock Wave Turbulent Boundary Layer Interaction with Bleed Through Normal and Slanted Slots," AIAA Paper 93-2155, June 1993.